Astron. Astrophys. 362, 646–654 (2000)

ASTRONOMY AND ASTROPHYSICS

Escape of VHE gamma-rays from close massive binary Centauri X-3

W. Bednarek

Department of Experimental Physics, University of Łódź, ul. Pomorska 149/153, 90-236 Łódź, Poland (Bednar@krysia.uni.lodz.pl)

Received 3 July 2000 / Accepted 31 August 2000

Abstract. We consider propagation of very high energy (VHE) gamma-rays in the radiation field of a massive star in the binary system Cen X-3, which has been reported as a source of gamma-ray photons in the GeV and TeV energies. VHE gamma-rays or electrons, injected by the compact object, should develop inverse Compton $e^{\pm}$ pair cascades. Based on the Monte Carlo simulations we predict the γ-ray spectra and the γ-ray light curves for the parameters of Cen X-3 system, and applying different models of injection of primary particles (monodirectional, isotropic, monoenergetic, power law). It is found that the gamma-ray spectra observed at different directions have different shapes and intensities. Interestingly, some gamma-rays may even escape from the binary system at directions which are obscured by the massive star, i.e. from the opposite side of the massive star to the location of the compact source of primary gamma-rays or electrons. We predict that the gamma-ray light curves, produced in the case of electron injection by the compact object in the Cen X-3 system, should have opposite tendencies for photons with energies above 100 MeV and above 300 GeV, i.e. the photon intensities increase with phase in the first case and decrease with phase in the second case. However the model with injection of primary electrons seems to be contrary to the reported modulation of the GeV γ-ray flux with the pulsar's period. The model with injection of primary photons allows such modulation with the pulsar's period, but predicts strong modulation of the TeV flux with the orbital period of the binary. Modulation of TeV emission with the orbital period was reported by the early Cherenkov observations, but was not confirmed by the recent, more sensitive observations by the Durham Mark 6 telescope.

Key words: stars: binaries: close – stars: individual: Cen X-3 – gamma rays: theory

1. Introduction

Massive binary systems are often considered as sites of high energy processes in which γ-ray production is expected. γ-rays in these systems may be produced in interactions of relativistic particles injected by a neutron star or a black hole (e.g. Bignami et al. 1977, Kirk et al. 1999), a shock wave created in collision of the pulsar and stellar winds (e.g. Harding & Gaisser 1990) or two stellar winds (e.g. Eichler & Usov 1993). Observations of these systems in GeV and TeV energies suggest that in fact this may be the case. For example in recent years the Compton GRO detectors have reported point sources with flat spectra coincident with some massive binaries e.g. Cyg X-3, LSI 303^{o}+61, or Cen X-3. Some positive detections of massive binaries by Cherenkov telescopes have been also claimed, although they were frequently accompanied by many negative reports (see for a review Weekes 1992, Moskalenko 1995). In the recent review on TeV observations only Cen X-3 has been mentioned as possible massive binary active at these energies (Weekes 1999).

These theoretical predictions and positive observations have stimulated analysis of propagation of VHE γ-rays in the anisotropic radiation fields of accretion disks around compact objects in massive binaries (Carraminana 1992, Bednarek 1993), and in the radiation fields of massive stars (e.g. Protheroe & Stanev 1987, Moskalenko et al. 1993, Moskalenko & Karakuła 1994). Recently we have performed Monte Carlo simulations of cascades initiated by monoenergetic γ-ray beams injected by a discrete source (probably a compact object) in the radiation field of a massive companion. Two massive binaries, Cyg X-3 (Lamb et al. 1977, Merck et al. 1995) and LSI 303^{o}+61 (van Dijk et al. 1996, Hermsen et al. 1977, Thompson et al. 1995), have been discussed in the context of this problem (Bednarek 1997).

Another massive X-ray binary, Cen X-3, containing a neutron star with a 4.8 s period in a 2.09 day orbit around an O-type supergiant, has been detected above 100 MeV by the EGRET detector on the Compton Observatory (Vestrand et al. 1997). There is evidence that the γ-ray emission at these energies is in the form of outbursts and is modulated with a 4.8 s period of the pulsar. Based on the observations in late 80's, two Cherenkov groups (Raubenheimer et al. 1989, Brazier et al. 1990, North et al. 1990) reported detection of positive signal at TeV energies from Cen X-3 at an orbital phase of ~ 0.75, which is modulated with a period of the pulsar. This emission has been localized by North et al. (1991) and Raubenheimer & Smit (1997) to a relatively small region between the pulsar orbit and the surface of a massive companion which may be the accretion wake or the limb of the star. More recently the Durham group has detected a persistent flux of γ-rays above 400 GeV on a lower level than previous reports (Chadwick et al. 1998, 1999a). No evidence of correlation with the pulsar or orbital periods has been found and

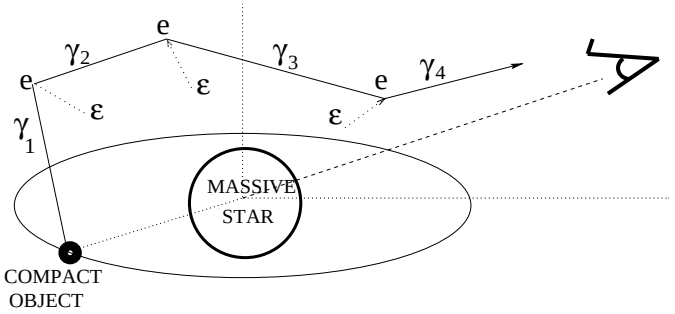

Fig. 1. Schematic picture of the cascade initiated by a primary gamma-ray (γ_1) in the radiation field of a massive star. The gamma-ray, injected by the compact object or produced by primary electron, creates an $e^{\pm}$ pair in the interaction with a soft star photon ε. The secondary $e^{\pm}$ pairs create secondary gamma-rays by scattering soft star photons (one of them is marked by γ_2). The next generation of gamma-rays may create further $e^{\pm}$ pairs; escape from the system (e.g. photon marked by γ_4); or collide with the star surface.

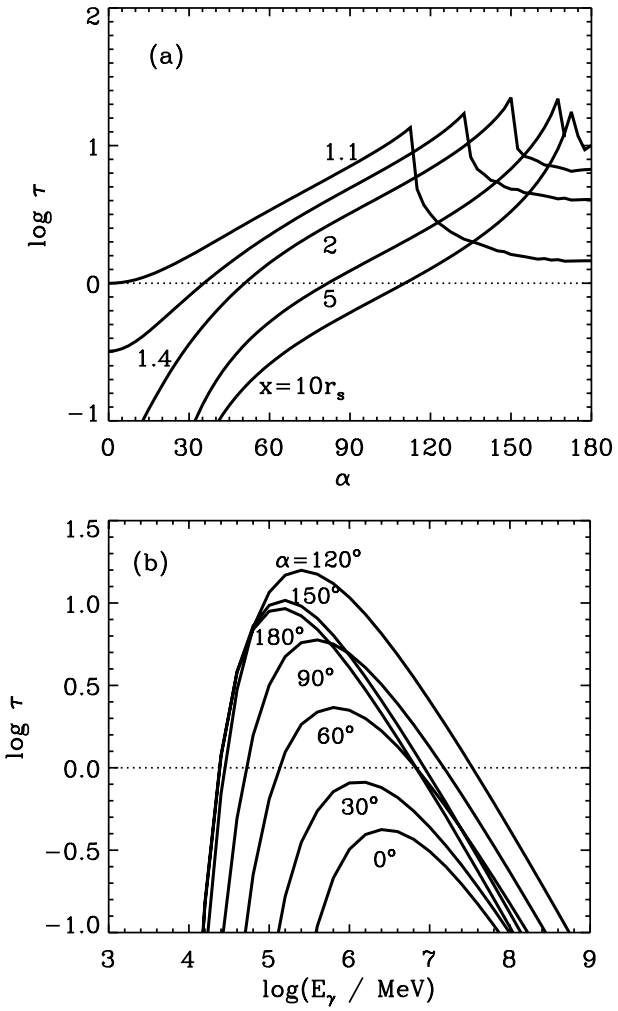

Fig. 2a and b. The optical depth for γ-ray photons with energies 10^6 MeV in the soft radiation field of the massive star in Cen X-3 system is shown as a function of the angle of injection of photons α, for different distances of the photon injection from the massive star equal to $x = 1.1, 1.4, 2, 5, 10$ radii of the star $r_{\rm s}$ **a**. The dependence of the optical depth on the photon energy, for fixed values of the angle α and the distance $x = 1.4r_{\rm s}$, is shown in **b**.

no evidence of correlation with the X-ray flux has been detected (Chadwick et al. 1999a,b).

The purpose of this paper is to compute the γ-ray light curves and γ-ray spectra escaping from the Cen X-3 system, assuming different geometries and energy distributions for primary electrons or photons injected into the radiation field of the massive star by a compact object. The geometry of the considered picture is schematically shown in Fig. 1. The γ-ray spectrum escaping from the system is a consequence of anisotropic cascades which initiate primary electrons or γ-ray photons in the thermal radiation of the massive star in Cen X-3. The results of computations are discussed in the context of observations of Cen X-3 in GeV and TeV energy ranges.

We assumed the following parameters for the massive binary Cen X-3: the radius of the O star $r_{\rm s} = 8.6 \times 10^{11}$ cm, its surface temperature $T_{\rm s} = 3 \times 10^4$ K (Krzemiński 1974), the binary star separation $a = 1.4r_{\rm s} = 1.2 \times 10^{12}$ cm, the inclination angle 70^o and a circular orbit since the known eccentricity of the binary is < 0.0008 (Fabbiano & Schreier 1977).

2. Propagation of VHE γ-rays in the radiation field of a massive star

In the previous paper (Bednarek 1997), we considered the propagation of monoenergetic γ-ray beams in the radiation field of a massive star in the case of two massive binaries: Cyg X-3 and LSI 303^o+61. We determined general conditions for which VHE γ-rays may initiate inverse Compton cascades (ICS) (see Sect. 2 in Bednarek 1997). The massive star in Cen X-3 system has also a high enough luminosity that VHE photons injected inside a few stellar radii should initiate a cascade. This expectation has been checked by computing the optical depth for γ-ray photons as a function of distance from the surface of the massive star, the photon energies, and the angle of injection α measured with respect to the direction determined by the place of photon injection and the center of the massive star. The optical depth has been computed as shown in Appendix A of Bednarek (1997). We have found that for the parameters of the massive star in the Cen X-3 system, the optical depth for photons injected at angles $\alpha > 30^o$ and at the distance $x = 1.4r_{\rm s}$ can be greater than one. If photons are injected closer to the massive star, then the optical depth can be greater than one for all injection angles (see curve for $x = 1.1r_{\rm s}$ in Fig 2a). The optical depth reaches maximum (characteristic cusps visible in Fig. 2a), for photons propagating in directions tangent to the massive star surface, i.e. at an angle $\alpha_\delta = \pi - \delta$, where δ is the angle intercepted by the massive star. For higher angles α, the optical depth is computed up to the moment of photon collision with the stellar surface and therefore it is lower than for α_δ.

As expected the optical depth for γ-ray photon reaches maximum at photon energies determined by characteristic energies of soft star photons (see Fig. 2b). Photons with energies below a few tens of GeV escape without significant absorption. There-

fore it is expected that cascade γ-ray spectra should show a break close to these energies.

3. Gamma-ray spectra from ICS cascade

Let us assume that a γ-ray photon is injected by the compact object which is in an orbit around the star with the parameters characteristic for Cen X-3 system. As we showed above these photons may create $e^{\pm}$ pair in collision with the soft star photon. We assume that secondary $e^{\pm}$ pairs are locally isotropised by the random component of the magnetic field. These pairs can next produce ICS γ-rays which may either escape from the system or collide with the massive star surface or interact with the next soft photon, initiating in this way an ICS cascade in the massive star radiation which is seen anisotropically with respect to the location of the injection place of the primary photons or electrons. The above described procedure is repeated for all cascade $e^{\pm}$ pairs up to the moment of their 'complete cooling', i.e. to the moment at which they are not able to produce γ-ray photons in ICS process with energies above a certain applied value which in our simulations is chosen as equal to 100 MeV. We also follow all secondary ICS γ-rays with energies above the threshold for $e^{\pm}$ pair production in the radiation of a massive star. The conditions for such cascades to occur and the details of the Monte Carlo simulations are presented in Bednarek (1997; note that Eq. (6) of that paper should have the form $P_1 = \exp(-\int_0^{l_\gamma} \lambda_{\gamma\gamma}^{-1}(E_\gamma, x_\gamma, \alpha_\gamma)dl)$).

In the subsections we discuss the results of calculations for different initial injection conditions, i.e. type, distribution, and spectra of primary particles.

3.1. Injection of monodirectional and monoenergetic photons or electrons

It is likely that high energy photons and/or electrons are injected by a neutron star (the compact object in the Cen X-3 system) in the form of highly collimated beams. Such beams may be formed in the outer gaps of pulsar magnetospheres (e.g. Cheng et al. 1986), in collisions of collimated protons escaping from the pulsar magnetospheres with the matter of an accretion disk (Cheng & Ruderman 1989), or they may emerge from regions of the magnetic poles of the neutron star (Kiraly & Meszaros 1988). In our simulations it is assumed that highly collimated beam of γ-rays with energy 10 TeV emerge from the distance $x = 1.4r_{\rm s}$ at a certain angle α, measured with respect to the direction determined by the center of the massive star and the compact object. In fact such a situation corresponds also to the case of highly collimated electron beams with comparable energy since at these energies electrons transfer almost all of their primary energy to a single γ-ray photon in ICS process because the scattering occurs in the Klein-Nishina domain.

We are interested in the spectra of secondary photons which escape from the above described type of cascade at a range of angles $\Delta\cos\theta = 0.2$. In Figs. 3, we show such secondary spectra for different injection angles of primary monoenergetic photons with energy $E_\gamma = 10^7$ MeV $\cos\alpha = 1$ (a), 0.5 (b), 0. (c), -0.5 (d), and -1 (e), observed at the range of angles: $\cos\theta = 0.8 \leftrightarrow 1.$ (dotted histograms), $0.4 \leftrightarrow 0.6$ (dashed), $0.2 \leftrightarrow 0$ (dot-dashed), $-0.6 \leftrightarrow -0.4$ (dot-dot-dashed), and $-1 \leftrightarrow -0.9$ (long-dashed). The cascading effects are the strongest (the highest numbers of secondary γ-rays) if the monoenergetic γ-ray beam is injected at the intermediate angles α (see thick solid histograms in Figs. 3, which show the secondary photon spectra integrated over all solid angles). This is a consequence of the highest optical depth for photons propagating at directions tangent to the massive star limb (curve for $x = 1.4r_{\rm s}$ in Fig. 2a). All secondary spectra are well described by a power law with the index ~ 1.5 at energies below ~ 10 GeV (as expected in ICS cascades with complete cooling of electrons). The photon intensities in these spectra are highest at the direction tangent to the limb of the massive star (dot-dot-dot-dashed histograms in Fig. 3). At higher photon energies (> 10 GeV), the spectra show characteristic cut-offs due to the absorption of secondary photons in the massive star radiation. The spectra recover at TeV energies with the intensities depending on the observation angle. The highest intensities are observed at small angles α for which the optical depth for TeV γ-rays is the lowest (see Fig. 2). In Fig. 3f, we compare the spectra escaping at fixed range of angles $\cos\theta = 0 \leftrightarrow 0.2$ but for different angles of injection of primary photons $\cos\alpha = 1.$ (dotted histogram), 0.5 (dashed), 0. (dot-dashed), -0.5 (dot-dot-dot-dashed), and $-1.$ (long dashed). It is clear that primary photons injected at directions of the highest optical depth ($\cos\alpha = -0.5 \leftrightarrow 0.$) produce secondary photons with the higher intensities than the ones injected at the directions of the lowest optical depth ($\cos\alpha = 1.$).

Note that in the type of cascade discussed here, the intensity of secondary photons observed at the direction of injection of primary photons is not completely dominated by these primary photons because of the large optical depths for the considered injection place ($x = 1.4r_{\rm s}$), and the isotropisation of secondary cascade $e^{\pm}$ pairs. Our assumptions on the propagation of photons in massive binaries are different than those applied in e.g. Kirk et al. (1999). These authors consider the binary systems in which the companion stars are largely seperated. In such systems only simple absorption effects of primary γ-rays may be considered since the secondary γ-rays, produced by secondary $e^{\pm}$ pairs, are not likely to interact again with the soft star photons.

3.2. Isotropic injection of monoenergetic photons or electrons

Monoenergetic photons and electrons can be isotropically injected into the binary system by young pulsars with strong pulsar winds. In fact, it is believed the pulsar winds are composed of relativistic electrons (positrons) which have typical Lorentz factors of the order $\sim 10^7$ (Rees & Gunn 1974). These electrons, if accelerated by the electric fields generated during magnetic reconnection in the pulsar wind zone, can be injected approximately isotropically. Therefore we consider the case of isotropic injection of photons or electrons with energies 10 TeV. If only 10 TeV electrons are injected, they should produce photons with comparable energies in a single scattering as mentioned

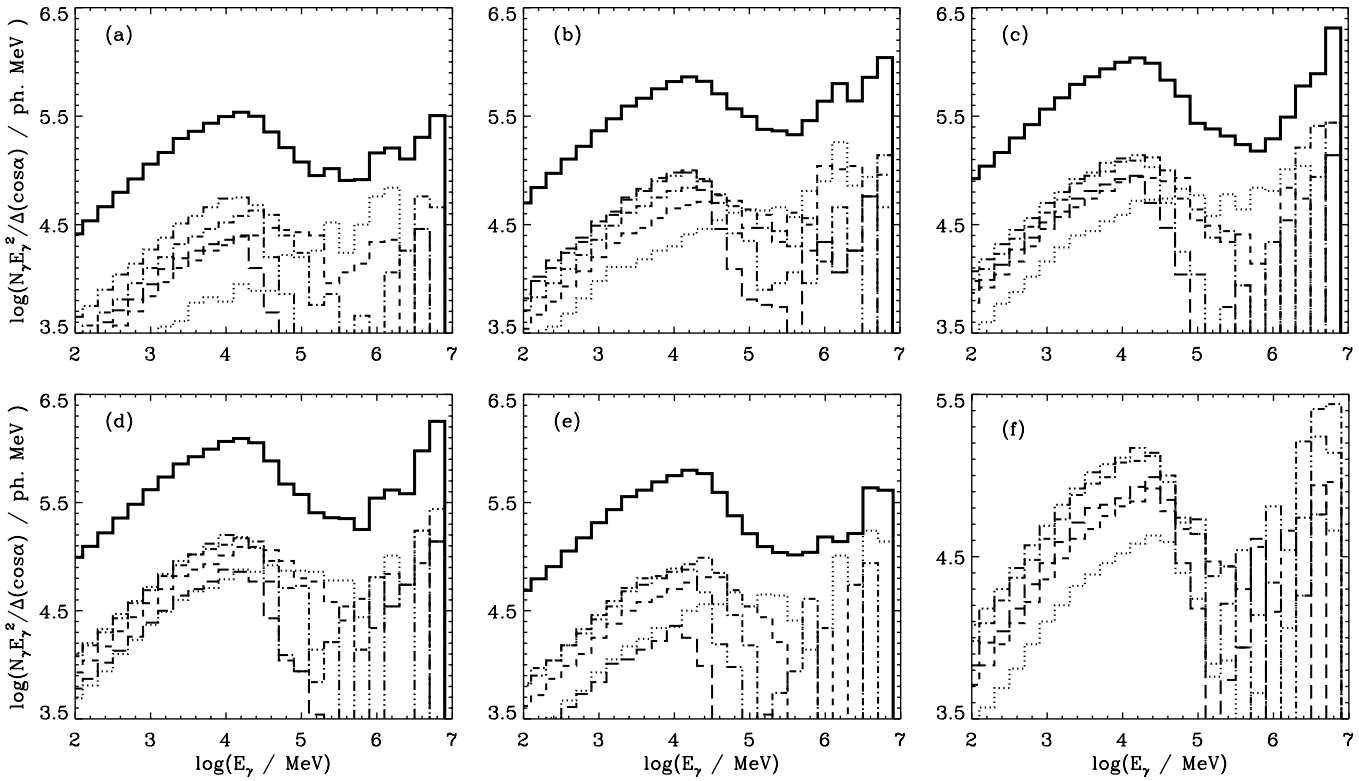

Fig. 3a–f. The secondary spectra of escaping γ-rays from the binary system with Cen X-3 parameters, in the case of injection of monodirectional and monoenergetic primary photons with energy 10^7 MeV. The spectra are shown for different angles of injection of primary γ-rays: $\cos\alpha = 1$ **a**, 0.5 **b**, 0. **c**, -0.5 **d**, and -1 **e**, within the range of observation angles: $\cos\theta = 0.8 \leftrightarrow 1.$ (dotted histograms), $0.4 \leftrightarrow 0.6$ (dashed), $0.2 \leftrightarrow 0$ (dot-dashed), $-0.6 \leftrightarrow -0.4$ (dot-dot-dashed), and $-1 \leftrightarrow -0.9$ (long-dashed). The thick solid histogram shows the secondary γ-ray spectrum integrated over all sphere. In figure **f** we compare the spectra escaping at fixed range of angles $\cos\theta = 0 \leftrightarrow 0.2$ in the case of different angles of injection of primary photons $\cos\alpha = 1.$ (dotted histogram), 0.5 (dashed), 0. (dot-dashed), -0.5 (dot-dot-dot-dashed), and $-1.$ (long dashed).

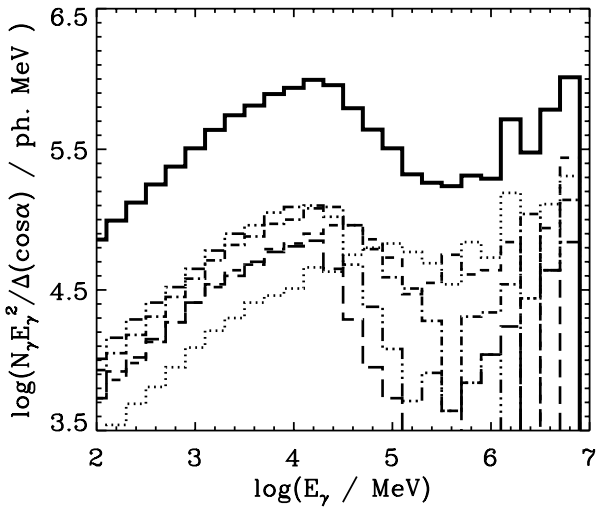

Fig. 4. The gamma-ray spectra escaping from the Cen X-3 binary system after cascading in the soft radiation field of the massive star in the case of isotropic injection of monoenergetic γ-ray photons with energy $E_\gamma = 10^7$ MeV. The secondary photon spectra are observed at a range angles: $\cos\theta = 0.8 \leftrightarrow 1.$ (dotted), $0.4 \leftrightarrow 0.6$ (dashed), $0 \leftrightarrow -0.2$ (dot-dashed), $-0.6 \leftrightarrow -0.4$ (dot-dot-dot-dashed), $-1 \leftrightarrow -0.8$ (long-dashed). The full thick histogram shows the secondary spectrum summed over all sphere.

above. The secondary photon spectra, produced in cascades under such initial conditions, are shown in Fig. 4 for different range of observation angles defined by: $\cos\theta = 0.8 \leftrightarrow 1.$ (dotted), $0.4 \leftrightarrow 0.6$ (dashed), $0 \leftrightarrow 0.2$ (dot-dashed), $-0.6 \leftrightarrow -0.4$ (dot-dot-dot-dashed), $-1 \leftrightarrow -0.8$ (long-dashed). The photon intensities observed at directions defined by very small angles θ and directions tangent to the massive star limb behave differently in different energy ranges. The intensities of GeV photons are highest for directions tangent to the stellar limb and lowest for small angles. This is contrary to what is observed at TeV energies. Note that a significant amount of secondary photons emerges also at the range of angles $\cos\theta = -1 \leftrightarrow -0.8$. This is on the opposite side of the massive star to the location of the compact source of primary photons and/or electrons (directions obscured by the star!). Therefore, the soft radiation of a luminous star may work as a kind of lens for high energy γ-ray photons causing the *focusing of very high energy photons*.

3.3. Isotropic injection of electrons with the power law spectrum

We consider also the case of the isotropic injection of electrons with a power law spectrum. Such electrons can be accelerated at the shock front created by the collision of the pulsar wind with

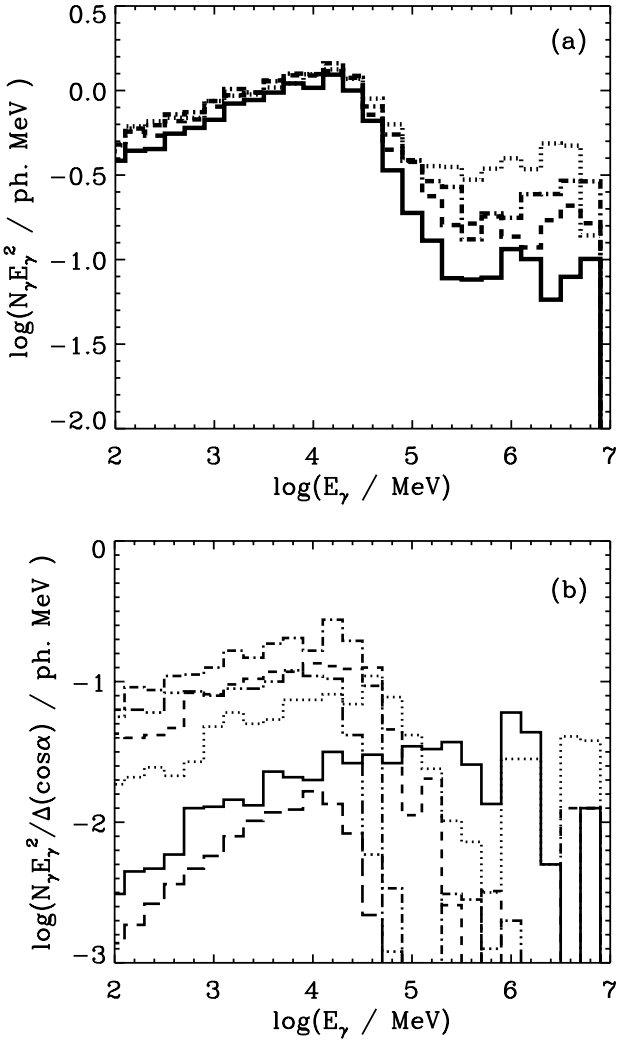

Fig. 5a and b. The γ-ray spectra observed from the Cen X-3 system in the case of isotropic injection of primary electrons with the power law spectrum and spectral index -2. The spectra integrated over all solid angle are shown in **a** for different distances of the point source of primary electrons from the massive star: $x = 1.4r_{\rm s}$ (full histogram), 2 (dashed), 3 (dot-dashed), and $5r_{\rm s}$ (dotted). The secondary γ-ray spectra escaping at different range of angles of observation: cos$\theta = 0.8 \leftrightarrow 1$ (full histogram), $0.4 \leftrightarrow 0.6$ (dotted), $0 \leftrightarrow 0.2$ (dashed), $-0.4 \leftrightarrow -0.2$ (dot-dashed), $-0.8 \leftrightarrow -0.6$ (dot-dot-dot-dashed), $-1 \leftrightarrow -0.8$ (long-dashed) are shown in **b**.

the surrounding matter as proposed in the model by Kennel & Coroniti (1984). It is assumed that electrons have a power law spectrum with index -2 (as expected from the theory of acceleration in strong shocks). They are injected from the discrete source orbiting the massive star in Cen X-3. In the binary system the shock may form relatively close to the compact object because the pulsar in Cen X-3 is relatively slow, and the density of the surrounding plasma inside the binary system is high.

The results of calculations of the secondary photon spectra escaping from ICS cascade, after integration over all solid angles, are shown in Fig 5a for different distances of the discrete source of primary electrons from the massive star. The results show that the integrated spectra in the energy region below ~ 10 GeV do not depend significantly on the location of the injection distance (in the range from the surface up to $5r_{\rm s}$). This effect may result from our assumption on the local capturing of secondary $e^{\pm}$ pairs by the random magnetic field. If the dominant magnetic field has ordered structure inside the binary then the propagation effects of pairs may be important. Such a more complicated cascade scenario is out of the scope of this paper and will be discussed in future work. The photon intensity decreases drastically at TeV energies for injection distances closer to the massive star surface.

We investigate also the dependence of the shape of the escaping spectrum of secondary γ-rays on the observation angle θ, for distance of injection $x = 1.4r_{\rm s}$ (see Fig. 5b). The features of these angular dependent spectra are similar to these ones described above for monoenergetic injection of electrons. The highest intensities at TeV energies are observed at small angles θ and the lowest intensities at directions behind the massive star. The highest intensities at GeV energies are for directions tangent to the massive star limb and the lowest for small angles and at directions obscured by the massive star.

3.4. Isotropic injection of photons with the power law spectrum

Finally we discuss the case of the isotropic injection of photons with a power law spectrum and spectral index -2. We show in Figs. 6 the spectra of escaping γ-rays for different distances of the injection place from the massive star (Fig. 6a) separately, the escaping spectra of primary γ-rays and secondary γ-rays for the injection place at $x = 1.4r_{\rm s}$ (Fig. 6b) and the angular dependence of secondary γ-ray spectra on the observation angle θ (Fig. 6c). General features of these spectra are very similar to the escaping spectra produced by electrons with a power law spectrum. The significant differences appear at low energies (below a few GeV) and at high energies (above ~ 1 TeV), and result from the contribution to the escaping spectrum from the primary γ-rays which do not cascade in the radiation of the massive star in Cen X-3. The escaping primary γ-rays flatten the spectrum at energies below a few 10^4 MeV (spectral index close to 1.9), and dominate the angle integrated spectrum at TeV energies.

4. Consequences for gamma-ray escape from Cen X-3

In the previous section we investigated general features of the γ-ray spectra escaping from the radiation field of a massive star. In order to have results of calculations which can be directly compared with the observations we compute the γ-ray light curves expected from the Cen X-3 system assuming that the compact object in this binary system injects γ-ray photons or electrons with a power law spectrum. The parameters of the Cen X-3 system, used in computations, are mentioned in the Introduction. Note that the orbit of the compact object is almost circular, so then the expected light curve should be symmetrical. Therefore we compute only the photon fluxes for the phases

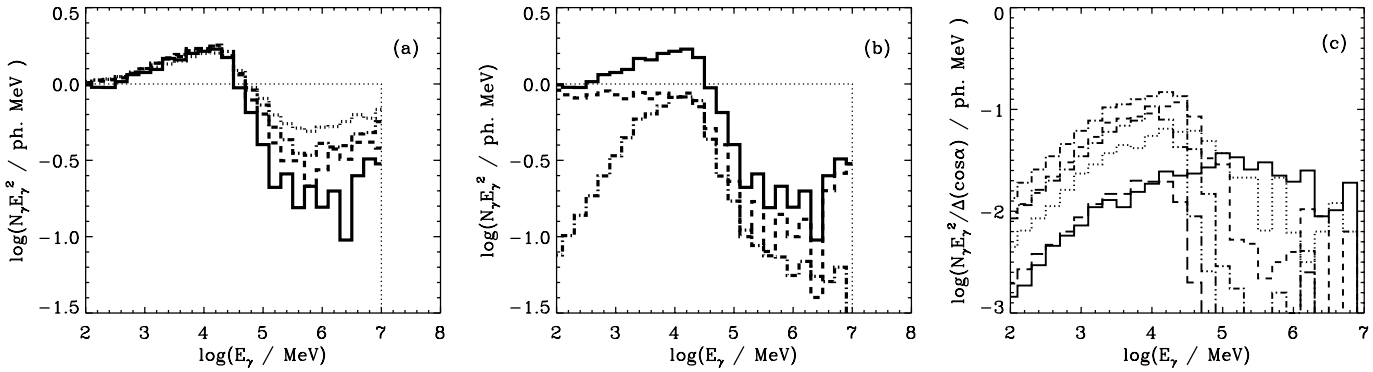

Fig. 6a–c. The spectra of γ-ray photons escaping from the Cen X-3 system in the case of isotropic injection of primary photons with a power law spectrum and spectral index -2, are shown in **a** for different distances between the center of the massive star and the injection place: $x = 1.4r_{\rm s}$ (full histogram), 2 (dashed), 3 (dot-dashed), and $5r_{\rm s}$ (dotted). The spectrum of photons injected by the compact object is marked by the thin dotted line. In **b** we show the photon spectra for the injection distance $x = 1.4r_{\rm s}$ which: escaped without interaction (dashed curve); are produced in the cascade (dot-dashed curve); and all photons escaping from the system (full curve). In **c** the gamma-ray spectra of secondary photons, in the case of injection at $x = 1.4r_{\rm s}$, are shown for different range of angles: $\cos\theta = 0.8 \leftrightarrow 1$ (full histogram), $0.4 \leftrightarrow 0.6$ (dotted), $0 \leftrightarrow 0.2$ (dashed), $-0.2 \leftrightarrow -0.4$ (dot-dashed), $-0.8 \leftrightarrow -0.6$ (dot-dot-dot-dashed), $-1 \leftrightarrow -0.8$ (long-dashed).

from 0 to 0.5, where the phase is measured from the side of the observer.

The γ-ray light curves of photons escaping from the system in the case of isotropic injection of electrons (or positrons) with a power law spectrum and spectral index -2 are shown in Figs. 7a,b for photons with energies above 100 MeV, i.e. the EGRET energy range (a), and above 300 GeV, i.e. Cherenkov technique energy range (b). The results are shown for the cut-offs in the spectrum of electrons at 10^7 MeV (full histogram) and at 10^8 MeV (dashed histogram). Note however, that the case with a cut-off at 10^8 MeV is shown only for comparison since it may not be completely right. Our assumption of the isotropization of secondary $e^{\pm}$ pairs with the Lorentz factors $\sim 10^8$ may not be justified in this case(see Eq. 3). The light curves show that the γ-ray flux should change drastically during the ~ 2.09 day orbital period of the system by at least an order of magnitude. However the γ-ray light curves observed at different energy ranges behave completely differently. When the photon flux above 100 MeV increases from the phase 0 up to the eclipse of the compact object by the massive star, which occurs for the phase ~ 0.38, the photon flux above 300 GeV decreases. This is the result of the propagation of photons in the anisotropic radiation of a massive star as discussed in details in Sect. 3. In Fig. 8, we show the spectra of γ-rays which should be seen by the observer for different phases of the compact object: 0 (full histogram), 0.15 (dotted), 0.35 (dashed), and 0.5 (dot-dashed). The photon spectra above 100 MeV have similar shapes but different intensities. The spectra above 300 GeV differ significantly not only in the intensities but also in shape.

We have also computed the γ-ray light curves in the case of isotropic injection of primary photons with the power law spectrum and index -2 (see Fig. 9a,b). Specific histograms in these figures show the light curves for all escaping γ-ray photons (full histograms), primary photons which escape without cascading (dotted), and secondary photons produced in cascades (dashed). As expected the light curves for secondary photons in the case of injection of primary photons and electrons are very similar. However the contribution of escaping primary photons to the γ-ray light curves with energies above 100 MeV dominates the secondary photons. Altogether, the γ-ray light curves at energies above 100 MeV are very flat with a strong decrease for phases between $\sim 0.38 \leftrightarrow 0.62$ resulting from the eclipse condition. During the eclipse, the observer may only detect secondary photons produced in cascades (dashed histogram in Fig. 9b), but on the level of about an order of magnitude lower. The γ-ray light curves above 300 GeV do not differ significantly for the case of injection of primary photons or electrons (compare Figs 7b and 9b). The contribution of primary non-cascading photons dominates only for small values of the phase (dotted histogram in Fig. 9b). From these computations it becomes clear that investigation of the γ-ray light curves at photon energies above 100 MeV (but not above 300 GeV) should allow the determination between types of primary particles dominantly produced by the compact object, photons or electrons (positrons), provided that these particles are injected isotropically with a power law spectrum.

We also show in Figs. 10a,b the spectra of escaping photons for different phases of the compact object, separately for secondary cascade photons and for primary photons which escape without interaction. The photon spectral index below ~ 10 GeV for all escaping photons (primary plus secondary) varies with phase only over a relatively small range, from -1.8 to -2. The observed photon fluxes are almost constant. At TeV energies the spectra change drastically with the phase of the compact object, similarly to the above discussed case of the injection of primary electrons. Note that for phase 0.5 (corresponding to the total eclipse of the compact object by the massive star), only secondary photons at energies below ~ 10 GeV can be observed (Figs. 10a and b).

As we have discussed in the Introduction, Cen X-3 has been detected in the GeV and TeV energy range. The emission in the GeV energy range can be fitted by a power law with spectral in-

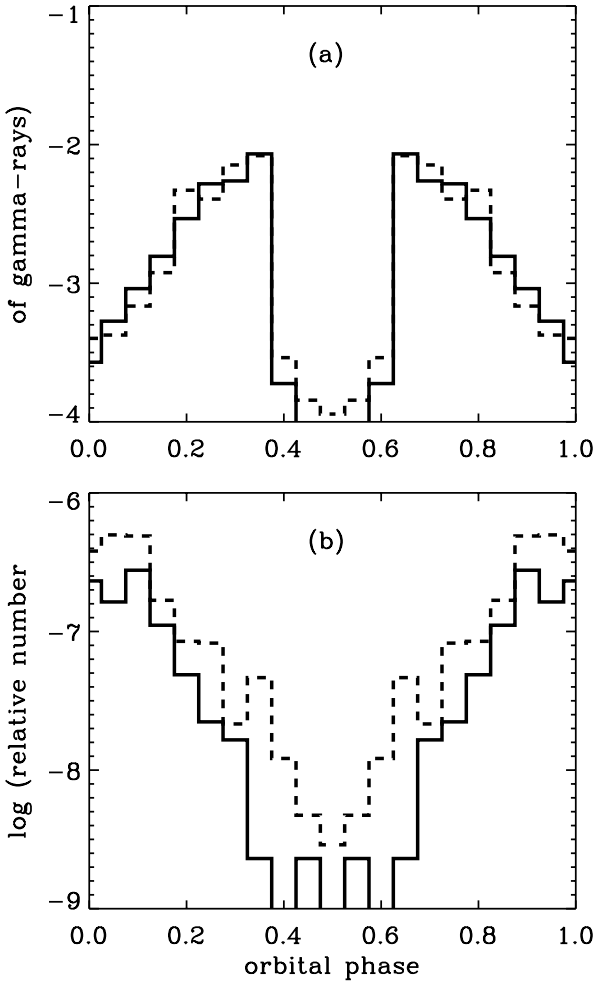

Fig. 7a and b. The light curves observed in γ-rays at inclination angle of the orbital plane of Cen X-3 system equal to 70^o at energies above 100 MeV **a**, and 300 GeV **b** in the case of isotropic injection of electrons with a power law spectrum with exponent -2. Specific histograms show the number of primary photons which escaped without interaction (dotted), secondary photons (dashed) and all photons (full).

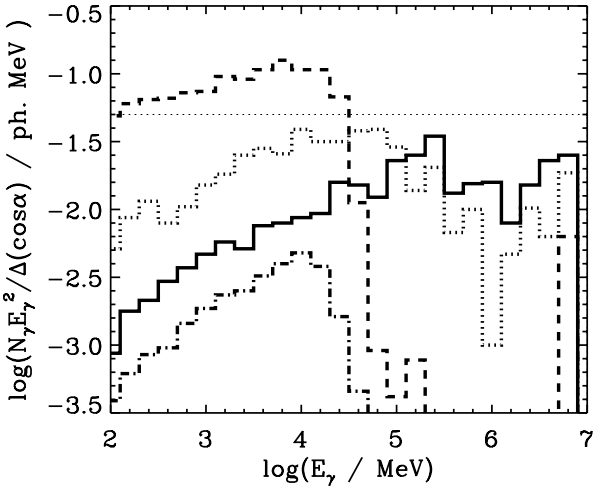

Fig. 8. Gamma-ray spectra observed from the Cen X-3 system at the inclination angle $i = 70^o$ for four different phases of the binary system 0. (full histogram), 0.15 (dotted), 0.35 (dashed), and 0.5 (dot-dashed) within the bin width equal to 0.1. The primary electrons, with a power law spectrum, exponent -2, and a cut-off at 10^7 MeV (a) and 10^8 MeV (b), are injected isotropically by the compact object.

dex -1.81 ± 0.37 (Vestrand et al. 1997). This index is consistent with our results for both discussed models of isotropic injection of primary photons or electrons with a power law spectrum and spectral index -2. However, the EGRET observations indicate modulation of the GeV emission with the pulsar's spin period, which should not be observed in the case of injection of primary electrons since the escaping photons at these energies were produced in the cascade process and the information on the pulsar period should disappear. Therefore the model with injection of primary electrons by the compact object seems not to work. The modulation with the pulsar period might be observed in the case of injection of primary photons from the compact object, provided that the secondary photons do not completely dominate the primary escaping photons. In fact, this is evident from our simulations (see Figs. 10a,b). However, as is seen in Fig. 9a, the photon flux, although constant through most of the phase range, should drop drastically during the eclipse of the compact object by the massive star. This feature has not been observed but also can not be rejected by the EGRET observations (Vestrand et al. 1997).

Cen X-3 has also been reported as a source of TeV photons modulated with the orbital period of the binary system by earlier, less sensitive Cherenkov observations (Brazier et al. 1990, North et al. 1990). Recent observations report that Cen X-3 is a source of steady emission above ~ 400 GeV (Chadwick et al. 1998). However modulation with the pulsar and orbital periods has not been found (Chadwick et al. 1999b). Our calculations show that in both models, injection of primary photons and injection of primary electrons by the compact object, the modulation of the signal with the orbital period should be very clear. On the other hand, the modulation with the pulsar period should not be observed because the secondary cascade photons determine the light curve in the case of injection of primary electrons and dominate or give a similar contribution to the light curve in the case of injection of primary photons (see dotted histogram in Fig. 9b).

5. Conclusion

We considered the cascade initiated by photons or electrons injected from the compact object in the radiation field of the massive companion in the Cen X-3 system, assuming that the secondary electrons are isotropised by the magnetic field in the binary. It is found that the features of the escaping photons from such massive binaries (the light curves, photon spectra as a function of the phase of the compact object) may allow the determination of which particles are injected by the compact object, i.e. photons or electrons. If the cascades are initiated by electrons then the escaping secondary cascade photons should not show features of modulation with the pulsar period. This

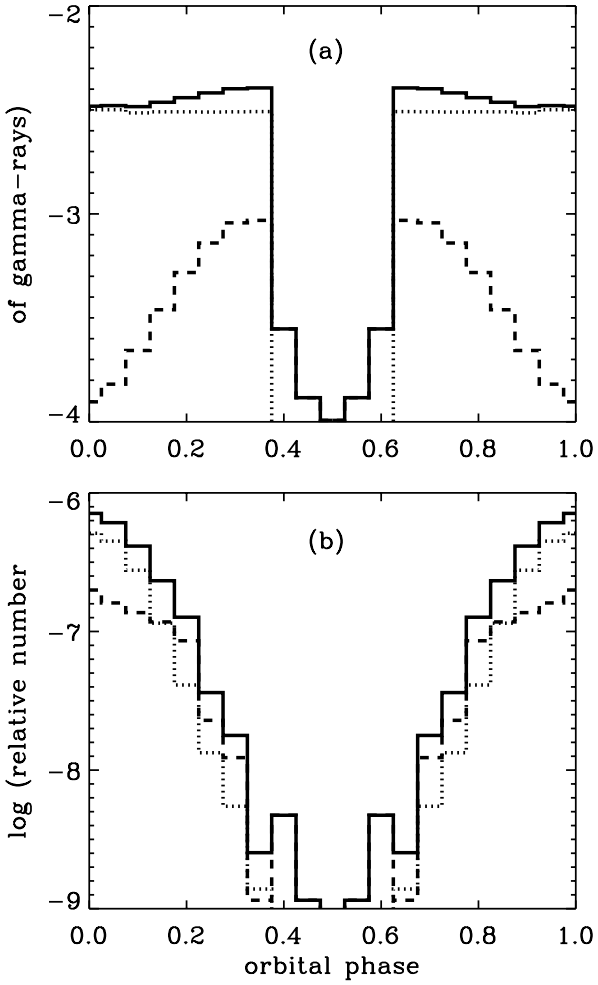

Fig. 9a and b. The γ-ray photon light curves observed at the inclination angle $70^{\rm o}$ to the orbital plane in Cen X-3 system at two energy ranges: above 100 MeV **a**, and above 300 GeV **b**. The primary γ-rays, with the power law spectrum with exponent -2 are injected by the compact object isotropically. Specific histograms show: the number of primary photons which escaped without interaction (dotted); the secondary photons (dashed); and all photons (full).

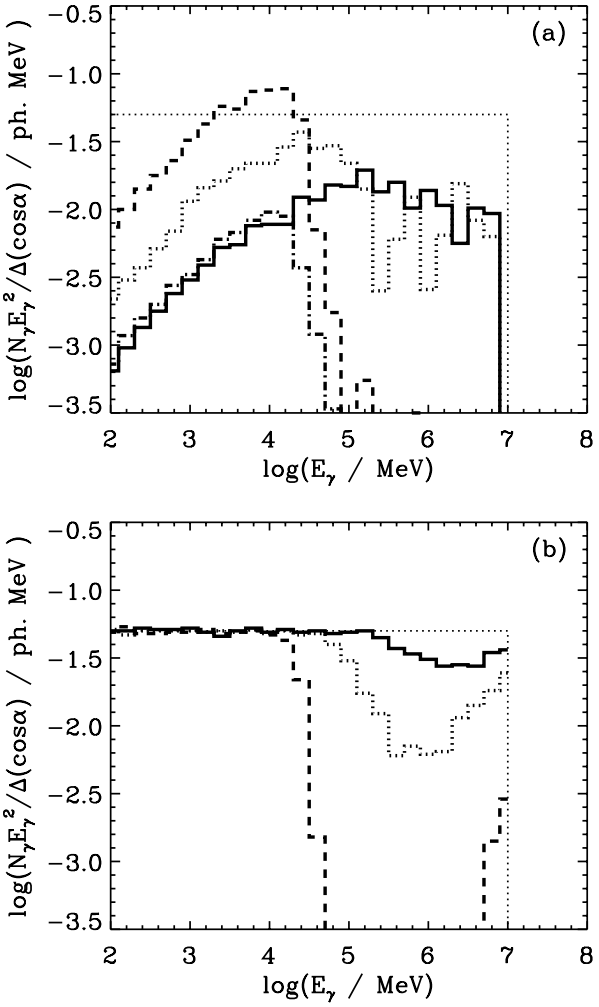

Fig. 10a and b. Gamma-ray spectra of secondary **a** and primary **b** photons escaping from the Cen X-3 system at the inclination angle $i = 70^o$ for four different locations of the compact source defined by the phase of the binary system: 0. (full histogram), 0.15 (dotted), 0.35 (dashed), and 0.5 within the bin width equal to 0.1. The primary gamma-rays are injected isotropically and have the power law spectrum with exponent equal to -2.

seems to be in contradiction with the observations of Cen X-3 at energies above 100 MeV. Therefore we reject such a model. If primary photons are injected isotropically with a power law spectrum and spectral index -2, then the spectrum of escaping photons at energies below $\sim$ 10 GeV is dominated, for most of the phases, by the primary non-cascading photons. Then, the modulation with the pulsar period can be observed. At TeV energies, the modulation of the photon flux with the 2.09 day binary period should be strong. The observation of modulation of the TeV signal with the orbital period of the system have been reported by earlier observations of Cen X-3 system (mensioned above) but not confirmed recently (Chadwick et al. 1999b). We think that this problem needs further investigation. The observations with the Mark 6 telescope had a tendency to cluster near orbital phases that had shown emission before, as commented in Chadwick et al. (1999b). Therefore the coverage of the orbit was not uniform. Also the presence of the 'high' and 'low' states observed in the system may have strong influence on the γ-ray light curve.

If the lack of modulation of the TeV photon flux with the Cen X-3 binary period is real, then a more complicated model has to be investigated. An extended source, e.g. a shock inside the binary system, injecting primary photons or electrons which initiate cascades in the soft radiation of a massive star should be developed. However such computations will require much more computing time in order to get satisfactory statistics, and therefore are left for future work.

In the present calculations we neglected the X-ray radiation field produced by the compact object. Its energy density $L_{\rm X} \approx 10^{38}$ erg s^{-1} (Giacconi et al. 1971) is comparable to the energy density of thermal photons from the massive star, so their photon density is a few orders of magnitude lower inside the volume of the binary system. We neglect also the heating effects of the

massive star by the X-rays coming form the compact object since the power emitted by the stellar surface is higher than the X-ray power falling on the massive star from the orbital distance of the compact object equal to 1.4 stellar radii. However note that X-rays, produced in the accretion disk around a compact object, i.e. close to the production site of primary photons, may absorb γ-rays if they are also produced close to the inner disk radius (see e.g. Bednarek 1993).

Acknowledgements. I thank the referee Dr. P. Chadwick for comments which helped to improve the paper and careful correction of the text of the paper. This work is supported by the Polish KBN grant 2P03C 006 128.

References

Bednarek, W. 1993, A&A 278, 307
Bednarek, W. 1997, A&A 322,523
Bignami, G.F., Maraschi, L., Treves, A. 1977, A&A 55, 155
Brazier, K.T., Carraminana, A., Chadwick, P.M. et al. 1990, Proc. 21st ICRC (Adelaide), vol. 2, p 296
Carraminana, A. 1992, A&A 264, 127
Chadwick, P.M., Dickinson, M.R., Dipper, N.A. et al. 1998, ApJ 503, 391
Chadwick, P.M., Lyons, K., McComb, T.J.L. et al. 1999a, ApJ 513, 161
Chadwick, P.M., Lyons, K., McComb, T.J.L., et al. 1999b, Proc. 26th ICRC (Salt Lake City), OG 2.4.9
Cheng, K.S., Ho, C., Ruderman, M.A. 1986, ApJ 300, 500
Cheng, K.S., Ruderman, M.A. 1989, ApJ 337, L77
Eichler, D., Usov, V. 1993, ApJ 402, 271
Fabbiano, G., Schreier, E. 1977, ApJ 214, 235
Giacconi, R., Gursky, E., Kellog, E., Schreier, E., Tananbaum, H. 1971, ApJ 167, L67
Harding, A.K., Gaisser, T.K. 1990, ApJ, 358, 561
Hermsen, W., Swanenburg, B.N., Bignami, G.F. et al. 1977, Nat 269, 494
Kennel, C.F., Coroniti, F.V. 1984, ApJ 283, 710
Kiraly, P., Meszaros, P., 1988, ApJ 333, 719
Kirk, J.G., Ball, L., Skjaeraasen, O. 1999, Astropart.Phys. 10, 31
Krzemiński, W. 1974, ApJL 192, L135
Lamb, R.C., Fichtel, C.E., Hartman, R.C., Kniffen, D.A., Thompson, D.J. 1977, ApJ 212, L63
Merck, M., Kanbach, G., Mayer-Hasselwander, H.A., Meintjes, P. 1995, Proc. 24th ICRC (Rome), v.2, p.190
Moskalenko, I.V. 1995, Space Sci.Rev. 72, 593
Moskalenko, I.V., Karakuła, S. 1994, ApJS 92, 567
Moskalenko, I.V., Karakuła, S., Tkaczyk, W. 1993, MNRAS 260, 681
North, A.R., Brink, C., cheng, K.S. et al. 1990, Proc. 21st ICRC (Adelaide), vol 2, p 275
North, A.R., Raubenheimer, B.C., Brink, C. et al. 1991, Proc. 22nd ICRC (Dublin), vol. 1, p 340
Protheroe, R.J., Stanev, T. 1987, ApJ 322, 838
Raubenheimer, B.C., North, A.R., De Jager O.C., Nel, H.I. 1989, ApJ 336, 349
Raubenheimer, B.C., Smit, H.J. 1997, Astropart.Phys. 7, 63
Rees, M.J., Gunn, J.E. 1974, MNRAS 167, 1
Thompson, D.J., Bertsch, D.L., Dingus, B.L. et al. 1995, ApJS 101, 259
van Dijk, R., Bennett, K., Bloemen, H. et al. 1996, A&A 315, 485
Vestrand, W.T., Sreekumar, P., Mori, M. 1997, ApJ 483, L49
Weekes, T.C. 1992, Space Sci. Rev. 59, 314
Weekes, T.C. 1999, in Proc. "GeV-TeV Astrophysics Toward a Major Atmospheric Cherenkov Telescope VI", Snowbird, Utah, in press, astro-ph/9910394